Image analysis of platelet derived growth factor receptor-beta (PDGFRβ) expression to determine the grade and dynamics of myelofibrosis in bone marrow biopsy samples

Running title: PDGFRβ expression in myelofibrosis – image analysis

Judit Bedekovics1, Szilvia Szeghalmy2, Lívia Beke1, Attila Fazekas2, Gábor Méhes1

1 Department of Pathology, Medical and Health Science Center

2 Department of Computer Graphics and Image Processing, Faculty of Informatics

University of Debrecen, Debrecen, Hungary

Corresponding author:

Gábor Méhes MD, PhD

Department of Pathology

University of Debrecen

Nagyerdei krt. 98.

H-4032 Debrecen, Hungary

Phone/Fax: +36 52 255 245

E-mail: gabor.mehes@dote.hu

Keywords: PDGFRβ, myelofibrosis, bone marrow

Abstract

Background: Myelofibrosis (MF) is characterized by accumulation of stromal cells and extracellular matrix. Progression of fibrosis is an important clinical issue and monitoring is required for new therapeutic approaches. Currently the quantification is based on semi-quantitative evaluation of reticulin silver stained slides. We recently reported that platelet derived growth factor receptor beta (PDGFRβ) expression in fibroblasts is a useful marker of stromal activation. PDGFRβ expression based scores represent significant differences in different myelofibrosis grade which provides optimal source of quantification. In this study slide based measurements were performed in order to support correlations of PDGFRβ expression with MF grade.

Methods: Scanned image tiles from 79 bone marrow samples (BM) with different myelofibrosis grades were evaluated for PDGFRβ-related IHC parameters. Following the determination of immunopositive (brown component) and total area (region of interest) of the BM, PDGFRβ related image parameters were defined and evaluated in comparison to the classical reticulin based grading.

Results: Eight PDGFRβ expression related image parameters showed excellent correlation with the MF grade (correlation coefficient ranging between 0.79 and 0.83) and with PDGFRβ score (0.76-0.87). Despite the significant sample heterogeneity the parameters showed significant differences between fibrotic and non-fibrotic cases and between mild and advanced fibrosis. Distribution of values within a particular specimen emphasizes the heterogeneity of bone marrow involvement which may cause difficulties in semi-quantitative methods.

Conclusions: Our results clearly demonstrated the correlation between myelofibrosis and PDGFRβ expression considering all relevant areas in BM samples. This method provides good basis for follow-up comparison of the fibrotic samples.

Keywords: PDGFRβ expression in myelofibrosis, bone marrow biopsy, myeloproliferative neoplasia, digital image analysis

Introduction

Myelofibrosis (MF) is a disorder of the bone marrow characterized by the accumulation of stromal cells and fibrous extracellular matrix which has an adverse effect on the hematopoietic activity (8). In the majority of the cases the pathologic mechanism including toxic, inflammatory or neoplastic processes is well known. MF usually occurs in advanced phases of myelodysplasia and myeloproliferative neoplasia while some clonal myeloproliferations are dominated by stromal fibrosis following a prefibrotic phase (primary myelofibrosis) (10, 19).

Classically, the status of the BM and the degree of the fibrotic process is determined by histological evaluation in BM trephine biopsies using reticulin silver staining (also named as Gomori's staining) (5). This highlights reticulin and collagen fiber deposition and is traditionally applied as a gold standard to determine the MF grade by demonstrating the actual amount of stromal fibers produced by stimulated fibroblasts (18). Accordingly the activation and proliferation of non-clonal fibroblasts is an important early event during the generation of MF. Fibroblast activity and collagen synthesis is under the control of tissue growth factors, such as transforming growth factor beta (TGF-beta) and platelet derived growth factor (PDGF) (3, 14). The latter is produced by bone marrow megakaryocytes and stored in the alpha granules of platelets to act physiologically as a cytokine mediator and initiator of tissue reparation. PDGF receptors (PDGFR) are members of the membrane tyrosine kinase family. Homo- or heterodimers are composed of the subunits PDGFRα and PDGFRβ (6, 7). The distribution of the PDGF receptor subunits on the surface of different kinds of cells shows lineage dependent variability. PDGFRβ acts as a strong activator of fibroblast proliferation upon ligand binding (12). As demonstrated by our previous study (2) PDGFRβ subunit was expressed by a limited set of mesenchymal cell types in the normal bone marrow. In

physiological conditions PDGFRβ positive stromal cells can be detected in the adventitial layer of vessel, in the endosteal layer of bone trabecules and further small amounts of scattered cells can be found in the intertrabecular bone marrow spaces. The distribution of the PDGFRβ positive fibroblasts suggests that these cells are parts of the vascular and osteoblastic hematopoietic niche. In bone marrow fibrosis the number of PDGFRβ positive cells massively increases. Using an immunohistochemistry based semi-quantitative scoring system presented earlier (2), strong correlation could be established between the amount of PDGFRβ positive cells (score 0-3) and the grade of myelofibrosis (grade 0-3). Both the PDGFRβ score which represents the number of fibroblasts and the MF grade which highlights the amount of the produced fiber show a wide spectrum within the bone marrow. This inhomogeneity of the mesenchymal reaction is not reflected properly in semi-quantitative methods.

In the present work we aimed the evaluation of PDGFRβ expression in BM slides using image analysis for the accurate and numeric expression of the immunopositivity. To evaluate different receptor related image parameters, a recently described image analysis algorithm was used (16), which allowed us to define the "region of interest" (intertrabecular hematopoietic area) in the complexity of the bone marrow biopsies. Within the region of interest the immunopositive areas (brown objects) were defined and characterized by different parameter settings. We assessed the correlation between the PDGFRβ expression related image parameters and the conventional MF grade, determined by reticulin silver staining in 42 bone marrow samples and repeated these analyses in further 37 samples which was not included in the initial pilot set of the study. To objectively demonstrate changes in the PDGFRβ expression during disease follow-up, serial samples taken from the same patients were selected from the latter group for further investigations.

Materials and methods

Bone marrow samples

Altogether seventy-nine trephine biopsy BM samples were selected with different degrees of myelofibrosis determined by the classical reticulin silver staining. All bone marrow specimens were taken at the Hematology Unit of the University of Debrecen for diagnostic purpose.

A pilot set of 10 non-pathologic and 32 pathologic samples from patients with the diagnosis of myeloproliferative neoplasia (14) or myelodysplastic syndrome (18) were selected, representing all stages of myelofibrosis. This pilot set was used for method development and for the selection of the image parameters. The correlation between PDGFRβ related image parameters and established semi-quantitative methods (MF grade and PDGFRβ score) and the spatial distribution of the parameters in samples with different MF grades was evaluated. To validate this method further 37 bone marrow samples with the diagnosis of myeloproliferative neoplasia were selected and evaluated in the same way.

To objectively demonstrate progressive changes in the PDGFRβ expression in follow-up cases with myeloproliferative neoplasia, serial bone marrow samples taken from different time points from the same patients were selected for further investigation.

Trephine biopsies were fixed for 24 hours in 4% phosphate buffered formaldehyde and decalcified for 48 hours in 1% EDTA. Following tissue processing and paraffin embedding 4um thick slides were cut for further stainings.

Reticulin silver staining

Gomori's reticulin staining was done according to the routine protocol. Slides were incubated in $KMnO_4$ dilution (0,5%), 1-3% solution of potassium metabisulfite, 2% solution

of ferric ammonium sulphate for 3 minutes, fresh made solution of silver for 1 minute, 4% solution of formalin for 5 minutes, and 0,1-0,2% solution of gold chloride. Every step was followed by distilled or tap water flushing. After the silver impregnation slides were dehydrated and covered with a cover-glass. The grade of reticulin staining was determined in the microscope according to the European Consensus on grading bone marrow fibrosis as follows (6). MF-0: faint fragments of reticulin fibers with no intersections; MF-1: loose network of elonged reticulin with intersections especially in perivascular areas; MF-2: diffuse and dens increase in reticulin with extensive intersections, with occasional bundles of collagen; MF-3: diffuse and dens increase in reticulin with extensive intersections, with coarse bundles of collagen also associated with apparent osteosclerosis. Evaluation was done by two experienced histologists simultaneously using double headed microscope to ensure the consistency of scoring. Control cases all showed MF0 grade. 5 of 32 pathological cases were classified into the MF0, 13 of 32 into the MF1, 7 of 32 into the MF2 group, while 7 of them showed MF3 grade fibrosis.

Immunohistochemistry

IHC was done as described earlier (2). To specifically demonstrate PDGFRβ positive cells, samples were incubated with anti-PDGFRβ (Abcam, ab-32570) primary monoclonal antibody at a dilution of 1:100 for one hour in a wet chamber. Antibody binding was visualized by the Dako EnVision FLEX/HRP and FLEX DAB3 Chromogen detection system (Dako) which was followed by hematoxylin counterstaining and coverage.

The PDGFRβ score was determined in the microscope according to a previously proposed scoring system (2). Score 0: no significant amounts of PDGFRβ positive stromal cells; score 1: isolated PDGFRβ positive fibroblasts (reticulum cells) present in the intertrabecular space; score 2: PDGFRβ positive fibroblasts forming a loose network by

partial intersections through long cellular processes; score 3: bands of PDGFRβ positive fibroblasts and their processes with frequent intersections forming a dense network. Evaluation was done by two experienced histologists simultaneously using double headed microscope to ensure the consistency of scoring. The pathologists were blinded to the results of the image analysis. 8 of the 10 control cases all showed PDGFRβ 0 score and 2 of them were score 1. 2 of 32 pathological cases were classified into the PDGFRβ 0, 8 of 32 into the PDGFRβ 1, 10 of 32 into the PDGFRβ 2 group, while 10 of them showed PDGFR beta 3 score expression.

Image acquisition and analysis

IHC stained slides were captured by the Pannoramic slide scanner device supplied by 3DHistech (Budapest, Hungary) using 20x magnification and a multicolor digital camera (Stingray F146C IRF Medical, Allied Vision Technologies, Stadtroda, Germany). Digitalized images were decompressed to obtain image tiles 768x768 in size which were used for evaluation. The total number of analyzed slides in the pilot set (42 cases) was 1437. The number of tiles per slide ranged between 6 and 147 (the mean tile number was 40.59) which varied according to the size and composition of the biopsy sample. The algorithm for digital measurement of PDGFRβ expression was described in detail earlier (16). Briefly, image processing was started with the generation of two separated layers (Figure 1.). The first layer defined IHC related brown staining or “brown layer” while the rest of the hematoxylin stained bone marrow parenchyma was determined as the “violet layer”. The brown layer was segmented from the original color images by pixel hue values (hue≤60 and 340≤hue). To distinguish the dark brown pixels representing specific antibody related staining in the cytoplasm of cells from the light brown pixels (unrelated background staining) background

correction was done. To find a suitable threshold we applied the Ramesh method on brown pixel saturation (12). The total of brown pixels (Figure 2. b) which had higher saturation as the specified threshold was considered as PDGFRβ positive. This purified brown layer consisted of brown objects different in size and shape, equivalent with separated or network-forming immunopositive cells, what was called brown component (Bc).

The IHC negative parenchyma defined as the violet layer was segmented by hue values between 160 and 320, saturation larger than 20. This did not cover fat tissue as it belonged to the white, empty areas of the slide. Besides the immunonegative cells in the hematopoietic area, the violet layer contained a lot of unrelated objects, such as bone trabecules, blood clots, connective or muscle tissue fragments. The latter unrelated tissue components were removed using an automated process. The differences in number and distribution of cell nuclei, and in the size of cytoplasm distinguished automatically unrelated tissues from hematopoietic areas (16). The violet layer finally contained only those immunonegative cells which belonged to the intertrabecular hematopoietic area. This purified violet layer was called the violet component (Vc).

The region of interest was the sum of the Bc and Vc which means that ROI (region of interest) consists of immunonegative and immunopositive cells of the intertrabecular spaces (Figure 2.). Selection of region of interest was performed automatically without manual changes. To validate the automated selection of useful area, ROI was selected in 419 tiles manually (300 randomly selected tiles, and 119 potentially problematic tiles) by an experienced pathologist and by the automated process as well. The specificity of the automated selection proved to be 97%. In order to characterize the IHC staining in each sample Bc and ROI were evaluated for a set of image parameters (Table 1.). The following parameters were evaluated in detail each tile. Number of objects: the total number of intertrabecular brown (immunopositive) objects which consist of PDGFRβ positive cells.

SumArea: the sum of the area (pixels) of all brown objects. SumPerimeter: the sum of the perimeter of all brown objects. (15). Further, we also considered the complexity of the brown objects by calculating the skeleton. SumSkeleton: the sum of the skeleton of all brown objects .The skeleton is the locus of the centers of all maximal inscribed hyper-spheres (i.e., discs and balls in 2D and 3D, respectively). An inscribed hyper-sphere is maximal if it is not covered by any other inscribed hyper-sphere (4). An additional parameter was the weighted Perimeter where the number of cross-points and end-points within the objects were considered (wPerimeter). The more complex network could be expected, the higher wPerimeter was calculated, even if the sumPerimeter itself was not increased due to the attachment of smaller objects.

Digital measurements resulted in representative numeric values reflecting individual specific features of the PDGFRβ staining pattern in each actual tile as a separated feature. Besides the total values (Sum), their highest fifty derivates (Top50 values) were also calculated for each tile of a case. In addition Top50 values were assessed for the whole slide as well. Relevant parameters were also normalized with the total intertrabecular marrow parenchyma (ROI).

Altogether 13 parameters were defined: SumArea, SumPerimeter, SumSkeleton, Number of objects, SumArea/ROI, SumPerimeter/ROI, SumSkeleton/ROI, Number of objects/ROI, Top50Area, Top50Perimeter, Top50Skeleton, Number of objects/Bc, wPerimeter/ROI.

Data from all image tiles were collected automatically without any manual changes. Before statistical analyses outlier values were removed. Altogether 13 parameters were evaluated, and only 2.5% of all tiles contained one or more outlier parameters. Outliers appeared mostly in cases with low amount PDGFRβ positive cells. Here, normal bone marrow vessels with immunopositive adventitial layer presenting as huge brown objects occur

in addition to the small scattered brown objects representing individual fibroblasts. Statistical analyses were performed before and after the exclusion of outliers and very similar results were obtained. Although the outliers did not significantly influence the results with the current set of cases, the exclusion of them may be important when we focus exclusively on a collection of pre-fibrotic bone marrow.

Statistical evaluation

Statistical evaluation and graphs were made using the GraphPad Prism software. Correlation between image parameters and classical MF grades was evaluated in detail. The Pearson r was calculated with 95% confidence interval, $p<0.05$ was considered to be a significant correlation, $r > 0.75$ was considered as strong correlation.

Results

Image processing and validation of PDGFRβ related measurements

Bone marrow biopsy specimens were captured using a slide scanner and the digitalized slides were decompressed into tiles with a uniform size of 768x768 pixels. These images covering the whole slides were applicable for a tile by tile image analysis process.

PDGFRβ related immunopositivity could be clearly represented in tiles of digitalized bone marrow slides independent from the cellular composition of the parenchyma (Figure 2.). A tile by tile quantitative analysis was performed for both the Brown component (Bc) and the region of interest (Bc + Vc) in separated image layers created on the basis of the color hue scales. Altogether 13 parameters were analyzed in digital slides and all of them showed significant correlation with the grade of MF and the PDGFRβ score. Eight of them showed

strong correlation (r>0.75) with the microscopic MF grade and PDGFRβ score as well (r>0.75) (Table 2.). These eight parameters were further assessed.

Image processing and statistical analyses were repeated in further 37 samples not included in the pilot set for validation purposes. Significant correlation of the eight image analysis parameters with MF grade and PDGFRβ score could be clearly validated. Spearman r ranged between 0.72 and 0.81 for MF grade and between 0.70 and 0.85 for PDGFRβ score.

PDGFRβ image parameters correlation with MF grade

Marked differences were identified in the different MF subgroups defined by the classical semi-quantitative method. To evaluate differences characteristic for MF grades, image parameters calculated for the whole slides were statistically analyzed (Figure 3). As expected, there was no measurable difference between the normal control BM and pathologic BM lacking fibrosis (MF0). In contrast, a gradual increase in all evaluated data sets could be seen from the MF0 to the MF3 grades in the diseased bone marrow. All of the eight selected parameters showed significant difference between MF0 and MF1 grades (P values between 0.012 and 0.047); M0 and MF2 grades (p<0.0001 in all settings); and MF0 and MF3 grades (p<0.0001 in all settings). All parameters of MF1 (mild fibrosis) vs. MF2 (intermediate reticulin fibrosis) cases showed robust differences with high significance levels (Top50Skeleton p=0.0012; Top50Perimeter p=0.0011; Top50Area p=0.0015; SumSkeleton/ROI p=0.0006; SumPerimeter/ROI p=0.0001; wPerimeter/ROI p=0.0149; SumArea/ROI p<0.0001; Number of objects/Bc p<0.0001). However, none of the applied parameters resulted in a statistically significant differences between pathologic MF2 and pathologic MF3 grades representing advanced fibrosis (Figure 3.).

There was no significant difference in the mean grade of myelofibrosis between the two pathological subgroups (MDS 1.60 vs. MPN 1.56 p=0.9322). None of the eight selected

PDGFR β related image parameters showed significant difference between these categories (P values between 0.2914 and 0.9957).

Comparison and graphical presentation of PDGFRβ expression in follow-up cases using immunohistochemistry based image analysis

The grade of myelofibrosis may vary remarkably within the bone marrow as regions around megakaryocyte clusters, perivascular and paratrabecular areas are usually more severely affected. PDGFRβ expression shows wide heterogeneity as well. Figure 4. shows results of measurements from 42 analyzed slides (n=1437 tiles) to demonstrate the continuous spectrum of values and the overlap between different MF subgroups for just two selected parameters (x= SumArea/ROI and y= Top50Area). Both parameters represent the area of immunopositive objects. Similarly wide distribution could be seen with the combination of those parameters which reflect the perimeter or the skeleton of immunopositive objects (diagrams not shown).

To see the utility of tile-based parameter measurement, serial follow-up bone marrow samples (not included in the pilot set of this study) were digitalized and analyzed from selected cases. Four parameters evaluated for objective sample comparison (SumArea/ROI; Number of objects/SumArea; Top 50 Area; Sum Perimeter/ROI) nicely reflected the dynamic of the fibrotic process. Figure 5. shows two examples for high-performance follow-up evaluation of bone marrow samples from patients with myeloproliferative neoplasia. In the first case the primary biopsy did not show fiber accumulation (MF grade 0), although a mild fibroblast activation was detected using PDGFRβ staining (PDGFRβ score 1). The follow up biopsy 12 months later presented advanced fibrosis (MF grade 2) and extended fibroblast proliferation (PDGFRβ score 2). There was a significant difference between the primary and follow-up

samples for all measured image parameters ($p<0.0001$) (Figure 5a). A second case presented with advanced fibrosis at the time of diagnosis (MF grade 2) which was accompanied by remarkable fibroblast accumulation as expected (PDGFRβ score 2). 4 years later, the follow up biopsy reflected that the fibrosis became more extended (MF grade 3), and so did the fibroblast accumulation (PDGFRβ score 3). Although tile based parameter values from the two samples were partially overlapping due to tissue heterogeneity, statistical analysis revealed significant differences in all of the four parameter combinations ($p<0.0001$) Figure 5b..

Discussion

PDGFRβ was described as a marker of activated mesenchymal cells, predominantly fibroblasts and was reported to have significant regulatory role in experimental fibrotizing conditions e.g. lung and liver fibrosis (1, 9, 11, 12). PDGFRβ expressing activated fibroblasts are responsible for matrix fiber production and therefore, their exact demonstration may provide insight into the dynamics of stromal reaction. Increase in PDGFRβ expression in the bone marrow related with the number of activated fibroblasts which correlated tightly with the grade of reticulin fibrosis using a semi quantitative four grade (0-3) microscopic scoring system (Spearman $r=0.83$; $p<0.0001$; $n=60$) (2). The proposed system – similar to the widely used reticulin evaluation scheme – considers mainly the mass and the complexity of the positive objects forming an increasing network in the progressive disease. Our result could be reproduced with the current measurements (Spearman $r=0.84$; $p<0.0001$; $n=79$), although the cases of the two studies showed partial overlap (23 cases were involved in both studies).

Although attempts for the automated assessment of reticulin fibrosis and osteosclerosis have been previously published showing good correlation with the semi-quantitative grading methods (17), these did not gain broad acceptance. In this study we describe a novel approach based on PDGFRβ immunohistochemistry and digitalized slide measurements. Tile-by-tile image analysis on scanned bone marrow sections strongly supported our earlier findings (2). To address PDGFRβ immunopositivity in digitalized slides several adjustments had to be performed. Bone marrow biopsy specimens very frequently contain other tissue elements such as fat, bone, skeletal muscle and connective tissue. To assess the extent and complexity of immunopositivity it was important to focus only the relevant intertrabecular spaces where hematopoiesis occurs. A major achievement of the presented analysis tool was the automated selection of the relevant measurement region (ROI) done by an algorithm carefully tested in a pilot setting.

The complexity of the immunopositive network formed by PDGFRβ expressing fibroblasts was addressed by the evaluation of a larger set of relevant image parameters. Related parameter values were established following the selection of relevant brown pixels for each tile. Area, number, perimeter, weighted perimeter and skeleton of brown objects were calculated) in each tiles. Total values (sum), derivates (top50 parameters) and normalized values (/ROI or /Bc) were calculated to qualify individual cases.

Area reflected mostly the actual mass of positive fibroblasts. The more positive cells presented the bigger was the area irrespective of the distribution of the cells. Perimeter and skeleton values addressed much more the overall distribution of the staining representing the varying density of cells and the increase in cell-to-cell connections characteristic for more advanced stage of fibrosis. These parameters can hypothetically reach a plateau level in advanced fibrosis when PDGFRβ positive cells form large, nearly homogenous areas. A

similar phenomenon is expected when the number of positive objects (activated fibroblasts) drops in late fibrosis.

Area, perimeter and skeleton values of brown objects are all supposed to be influenced by heterogeneity within the bone marrow parenchyma, therefore the total values of the individual tiles were calculated. Accordingly, significant correlation with the MF grade could be stated at the whole slide level (Table 2). Variety in sample size and cellularity made the normalization with the total intertrabecular hematopoietic area (ROI) necessary (Table 2). As the ROI did not include the fat tissue, values after normalization wit ROI were not further influenced by the cellularity. MF is characterized by the gradual increase of stromal cell mass starting from isolated mesenchymal cells. Even in advanced fibrosis with complex networks, scattered individual fibroblasts not communicating with the network are expected to be present. As this large number of brown objects with small area, perimeter, and skeleton may potentially cover features of progression, the highest 50 (Top 50) values of area, perimeter and skeleton were also considered. As a result, Top 50 parameter values demonstrated highly significant and strong differences between the MF grades.

Using the above mentioned PDGFRβ related image parameters we were able to demonstrate significant differences between individual MF grades. All of the 13 analyzed parameters were in correlation with the MF grade. Eight parameters (SumArea/ROI, SumPerimeter/ROI, SumSkeleton/ROI, wPerimeter/ROI, Top50Area, Top50Perimeter, Top50Skeleton, Number of objects/Bc) showed strong correlation (Spearman $r>0.75$) with MF grade and PDGFRβ score as well. We were able to validate significant correlation in a second set of bone marrow samples with 37 specimens stained for PDGFRβ. SumArea, SumPerimeter, SumSkeleton, Number of objects, Number of objects/ROI were in weak correlation with MF grade in initial testing so they were dropped.

On the basis of our studies, selected PDGFRβ related image parameters proved to be effective to distinguish bone marrow samples with myelofibrosis from the non-fibrotic group (all of the eight parameters in Table 2. comparing MF0 to M1-3) or to differentiate between mild and advanced fibrosis (all of eight parameters in Table 2. comparing MF1 to MF 2). Especially SumArea/ROI; Number of objects/Bc, SumPerimeter/ROI and SumSkeleton/ROI were applicable (p value ranges between <0.0001 and 0.0006). However, none of the applied image parameters represented clear differences between pathologic MF2 and pathologic MF3 grades (advanced fibrosis). It has to be mentioned that MF grades reflect the mass of fibers produced by fibroblasts, while PDGFRβ related parameters indicate the amount of newly generated fibroblast. It can be speculated that fibroblast activation and proliferation precedes fiber production in early lesions. In reverse, activated fibroblast highlighted by PDGFRβ may not be proportionally required in end-stage disease.

In the most advanced phase of myelofibrosis, PDGFRβ positive fibroblasts form a dense network which could be associated with the maximal grade of fibrosis if the process is fully developed. In our study only 6 of the 10 cases with PDGFRβ score 3 showed the most extended fiber accumulation (MF-3). In other cases the fibroblast accumulation reached a maximum level (PDGFRβ score 3) while the fiber accumulation was still in progress and the sample was classified as MF2 (3 cases) or MF1 (1 case).

Bone marrow heterogeneity is well known in myelofibrosis. The bone marrow parenchyma is not uniformly involved by the distribution of activated fibroblasts and extracellular matrix fibers. The classical MF grading is mainly based on the dominant changes occurring in the section while image measurements (depending on the parameters selected) more reflect the mean of all events irrespective of their distribution. From this perspective, it may be difficult to identify finer differences during follow-up studies using a four grade semi-quantitative system. The clinical need to assess the status of stromal activation more precisely

during patient follow-up is clear. Moreover, PDGFRβ based image analysis could be an objective tool to evaluate the therapeutic efficiency of new treatment protocols including e.g. JAK-2 inhibitors. Figure 5. demonstrates application on follow-up samples, where each dot represents parameters from a single tile. Although tile-based image parameter values showed a high variability within and an overlap between the serial samples, statistical calculations pointed to significant differences. The presented follow up cases give typical examples for the heterogeneous composition of bone marrow samples.

Although some of PDGFRβ related image parameters showed excellent correlation with the MF grade, mesenchymal activation related PDGFRβ expression was more extended then fiber accumulation in different MF subgroups. As fibroblast proliferation precedes fiber production, it can be hypothesized, that elevated PDGFRβ expression is useful for the prediction of MF progression. This issue can be especially interesting in pre-fibrotic cases or in cases with mild fibrosis, but it requires a statistical evaluation of a larger sample cohort.

The PDGFRβ expression related image analysis is a promising example for digital support of the evaluation of immunohistochemical reactions. Besides the appropriate selection of intertrabecular hematopoietic area in the complex bone marrow, the analysis of well defined parameters describing networks with different extension is also enabled. Based on the statistical analyzes eight parameters showed strong correlation with the semi-quantitative methods (SumArea/ROI, SumPerimeter/ROI, SumSkeleton/ROI, wPerimeter/ROI, Top50Area, Top50Perimeter, Top50Skeleton, Number of objects/Bc). As skeleton and perimeter provide similar information about the extension of the network, and the statistical analyzes could not reveal differences between them, it is not necessary to use both parameters for the same time. Finally, a combination of five parameters (SumArea/ROI, SumPerimeter/ROI, Top50Area, Top50Perimeter, Number of objects/Bc) can be proposed for the digital image analysis of bone marrow samples stained for PDGFRβ. We believe that

parameters introduced here are able to precisely characterize the extent and complexity of immunopositive objects. As such, this approach could also be used for similar immunostainings highlighting network-forming elements, e.g. stroma cells positive for tenascin.

In conclusion, PDGFRβ was found to be a practically useful stromal activation marker, also enabling automatic image analysis. Digital tile based evaluation of PDGFRβ immunostaining reflected significant differences in stromal activity and demonstrated intraparenchymal heterogeneity in different hematopathological conditions of the bone marrow.

Acknowledgement

The scientific work (infrastructural background) was supported by the TÁMOP- 4.2.2.A-11/1/KOV-2012- 0045 “Research network on vascular biology/medicine” project and the personal support provided by the TÁMOP 4.2.4. A/2- 11-1-2012-0001 „National Excellence Program – Elaborating and operating an inland student and researcher personal support system. The project was subsidized by the European Union and co-financed by the European Social Fund.

Conflict of interest statement

We declare that we have no conflict of interest.

References

1. Abdollahi A, Li M, Ping G, Plathow C, Domhan S, Kiessling F, Lee LB, McMahon G, Grone HJ, Lipson KE, Huber PE. Inhibition of platelet-derived growth factor signaling attenuates pulmonary fibrosis. J Exp Med 2005; 201 (6):925-935.

2. Bedekovics J, Kiss A, Beke L, Karolyi K, Mehes G. Platelet derived growth factor receptor-beta (PDGFRbeta) expression is limited to activated stromal cells in the bone marrow and shows a strong correlation with the grade of myelofibrosis. Virchows Arch 2013 Jul; 463(1):57-65.

3. Bonner JC. Regulation of PDGF and its receptors in fibrotic diseases. Cytokine Growth Factor Rev 2004; 15 (4):255-273.

4. Calabi L. A study of the skeleton of plane figures. Technical Report, Parke Mathematical Laboratories; 1965. 66 p.

5. Gomori G. Silver Impregnation of Reticulum in Paraffin Sections. Am J Pathol 1937; 13 (6):993-1002.

6. Funa K, Uramoto H. Regulatory mechanisms for the expression and activity of platelet-derived growth factor receptor. Acta Biochim Pol 2003; 50 (3):647-658.

7. Heldin CH, Westermark B. Mechanism of action and in vivo role of platelet-derived growth factor. Physiol Rev 1999; 79 (4):1283-1316.

8. Hoffman R, Rondelli D. Biology and treatment of primary myelofibrosis. Hematology / the Education Program of the American Society of Hematology American Society of Hematology Education Program 2007; 346-354. Epub 2007/11/21.

9. Ikura Y, Morimoto H, Ogami M, Jomura H, Ikeoka N, Sakurai M. Expression of platelet-derived growth factor and its receptor in livers of patients with chronic liver disease. J Gastroenterol 1997; 32 (4):496-501.

10. Kuter DJ, Bain B, Mufti G, Bagg A, Hasserjian RP. Bone marrow fibrosis: pathophysiology and clinical significance of increased bone marrow stromal fibres. Br J Haematol 2007; 139 (3):351-362.

11. Pinzani M, Milani S, Herbst H, DeFranco R, Grappone C, Gentilini A, Caligiuri A, Pellegrini G, Ngo DV, Romanelli RG, Gentilini P. Expression of platelet-derived growth factor and its receptors in normal human liver and during active hepatic fibrogenesis. Am J Pathol 1996; 148 (3):785-800.

12. Rajkumar VS, Shiwen X, Bostrom M, Leoni P, Muddle J, Ivarsson M, Gerdin B, Denton CP, Bou-Gharios G, Black CM, Abraham DJ. Platelet-derived growth factor-beta receptor

activation is essential for fibroblast and pericyte recruitment during cutaneous wound healing. Am J Pathol 2006; 169 (6):2254-2265.

13. Ramesh N, Yoo JH, Sethi IK. Thresholding Based on Histogram Approximation. Iee P-Vis Image Sign 1995; 142 (5):271-279.

14. Reilly JT. Pathogenesis of idiopathic myelofibrosis: role of growth factors. J Clin Pathol 1992; 45 (6):461-464.

15. Sonka M, Hlavac, V. Boyle, R. Image Processing Analysis and Machine Vision (3rd edition). CL-Engineering; 2007. 872 p.

16. Szeghalmy Sz, Bedekovics J, Mehes G, Fazekas A. Digital measurement of myelofibrosis associated platelet derived growth factor receptor ß (PDGFR ß) expression in bone marrow biopsies. CIT 2013; 21(1): 49-58.

17. Teman CJ, Wilson AR, Perkins S, L.Hickman K, Prchal JT, Salama ME. Quantification of fibrosis and osteosclerosis in myeloproliferative neoplasms: a computer-assisted image study. Leuk Res 2010; 34 (7):871-876.

18. Thiele J, Kvasnicka HM, Facchetti F, Franco V, van der Walt J, Orazi A. European consensus on grading bone marrow fibrosis and assessment of cellularity. Haematol 2005; 90 (8):1128-1132.

19. Wadleigh M, Tefferi A. Classification and diagnosis of myeloproliferative neoplasms according to the 2008 World Health Organization criteria. Int J Hematol 2010; 91 (2):174-179.

Table and figure legends

Table 1. Definitions of image parameters applied to describe PDGFRβ related immunopositive areas captured from digital slides.

** Relevant parameters were also used normalized with the total marrow parenchyma (region of interest, /ROI).*

Table 2. Correlation of image parameters representing PDGFRβ immunopositivity in scanned digital sections with myelofibrosis grade and PDGFRβ score determined by classical microscopy. PDGFRβ (Brown component = Bc) related parameters were ranked according to the correlation coefficients. Strong correlation was stated for the eight listed parameters (r>0.75).

Figure 1. Image analysis algorithm for the evaluation of platelet derived growth factor receptor beta (PDGFRβ) expression in digitalized bone marrow biopsy specimens.

Figure 2. Digital captures of PDGFRβ immunostained bone marrow samples representing a strong positivity in an MF2 case. A: Unprocessed digital image tile representing remarkable PDGFRβ expression in true colors. B: Segmentation of brown layer after background correction resulted in the PDGFRβ related brown component (Bc) which is the sum of high saturated brown pixels. Brown objects appear in different size. C: Segmentation of violet layer after automated removal of unrelated structures (bone trabecules) which results in purified violet layer called the violet component (Vc). D: The region of interest (ROI) was calculated (Bc + Vc) containing all relevant components of the cellular bone marrow parenchyma.

Figure 3. Mean values of PDGFRβ related image parameters in different grades of myelofibrosis (n=42). MF grade (0-3) was conventionally determined in the microscope following classical reticulin staining in normal (control) bone marrows and in different pathologic conditions associated with marrow fibrosis. *MF0 path* represent cases with established histopathological diagnosis lacking considerable amounts of myelofibrosis, potentially including prefibrotic bone marrows. (MF: myelofibrosis)

Figure 4. Distribution of SumArea/ROI and Top50 Area values in the total collection of tiles (n= 1437) measured in 42 slides. Specific MF grades are highlighted by dark dots while all tiles are represented in the background. Samples with different MF grades were impossible

to separate due to significant tissue heterogeneity but the gradual increase was obvious in accordance with PDGFRβ expression.

Figure 5. Follow-up analysis of bone marrow samples from sequential biopsies with progressive myeloproliferative neoplasia. Each dot represents values from a single tile, the follow up samples are indicated by different dot marking (blue = first biopsy, red = second biopsy).

Case 1 (left). Mild fibroblast activation (first biopsy, MF-0, PDGFRβ score 1) progressed to marked accumulation of stromal cells in the follow-up biopsy (second biopsy, MF-2, PDGFRβ score 2) which was clearly shown by significant changes of PDGFRβ related image parameters. The partial overlap between the tiles of the two samples can be explained by the uneven distribution of the fibrotic change within the bone marrow sample. Statistically significant difference could be revealed for all parameters.

Case 2 (right). Advanced fibrosis could be detected already at the time of histological diagnosis (first biopsy, MF-2, PDGFRβ score 2) which became more severe in a sample obtained 4 years later (second biopsy, MF-3, PDGFRβ score 3). Statistically significant difference could be revealed for all parameters between the initial and the follow up samples.

ROI: region of interest (Brown component + Violet component).

Table 1.

Parameter *	Definition
Number of objects	Number of immunopositive (brown) objects
SumArea	Sum of immunopositive pixels in all objects
SumSkeleton	Sum of the distance of skeletons calculated in immunopositive objects
SumPerimeter	Sum of immunopositive object perimeters
WPerimeter	Sum of immunopositive objects weighted perimeters (with the number of cross-points and endpoints)
Top 50 Area	Sum of pixels of the 50 immunopositive objects with the largest area
Top 50 Skeleton	Sum of the distances of 50 immunopositive objects with the largest skeleton distance
Top 50 Perimeter	Sum of the 50 immunopositive object with largest perimeters
/ROI	parameters normalized with the region of interest
/Bc	parameters normalized with the brown component

Table 2.

Parameter	Correlation with MF grade		Correlation with PDGFRβ score	
	Spearman-R	P-value	Spearman-R	P-value
PDGFRβ score	0,8578	< 0,0001	-	-
MF grade	-	-	0,8578	< 0,0001
SumArea/ROI	0,7956	< 0,0001	0,8669	< 0,0001
Number of objects/Bc	-0,7893	< 0,0001	-0,7594	< 0,0001
Sum Perimeter/ROI	0,7886	< 0,0001	0,8702	< 0,0001
wPerimeter/ROI	0,8233	< 0,0001	0,8473	< 0,0001
Sum Skeleton/ROI	0,7878	< 0,0001	0,8650	< 0,0001
Top 50 Area	0,8093	< 0,0001	0,7626	< 0,0001
Top 50 Perimeter	0,8237	< 0,0001	0,7898	< 0,0001
Top 50 Skeleton	0,8279	< 0,0001	0,7860	< 0,0001

Figure 1.

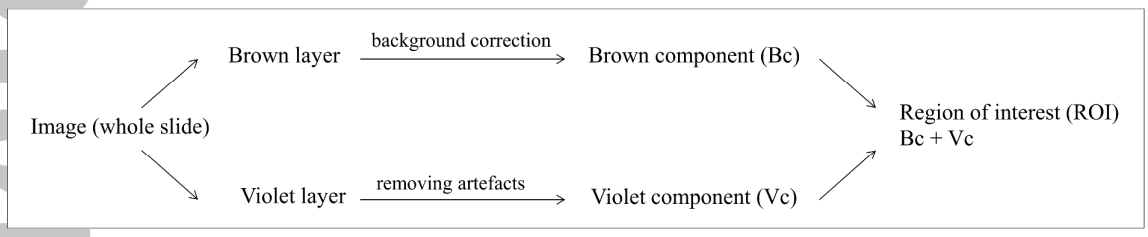

Figure 2.a.

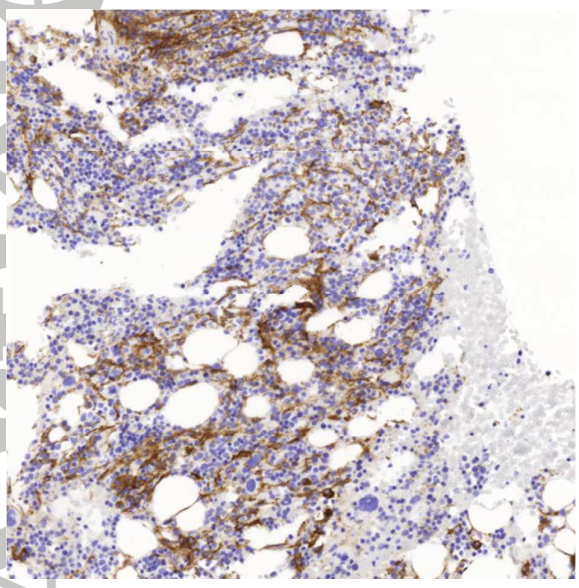

Figure 2.b.

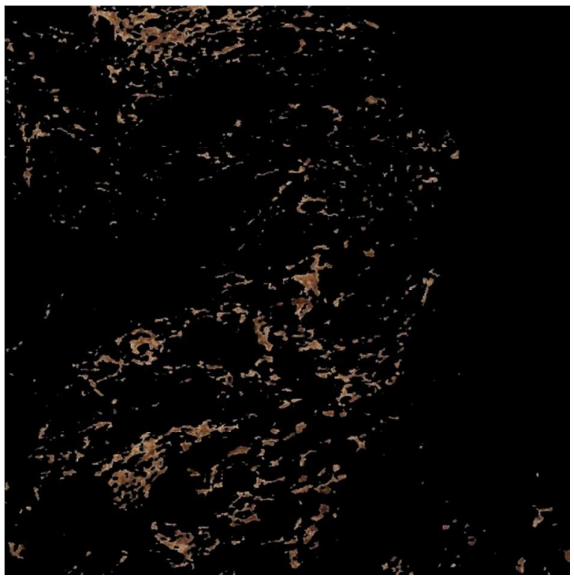

Figure 2.c.

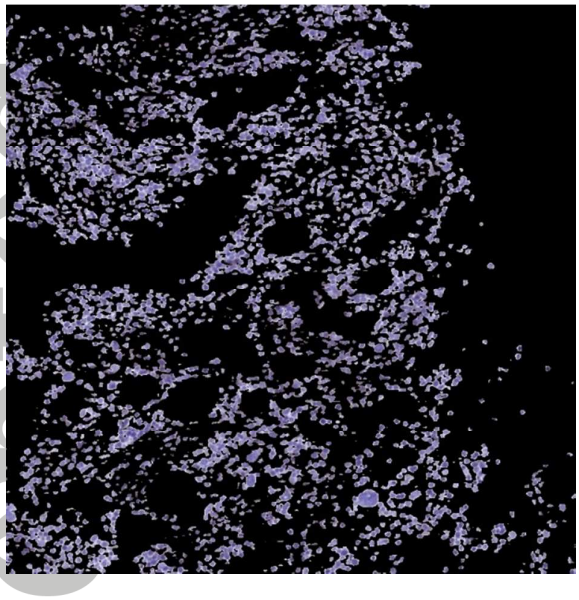

Figure 2.d.

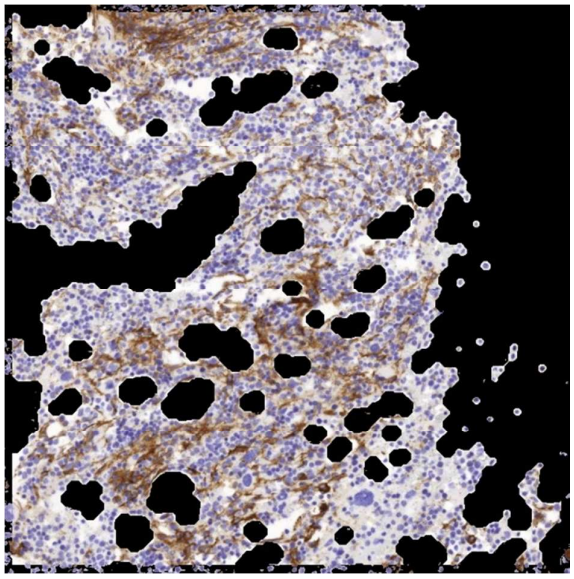

Figure 3.

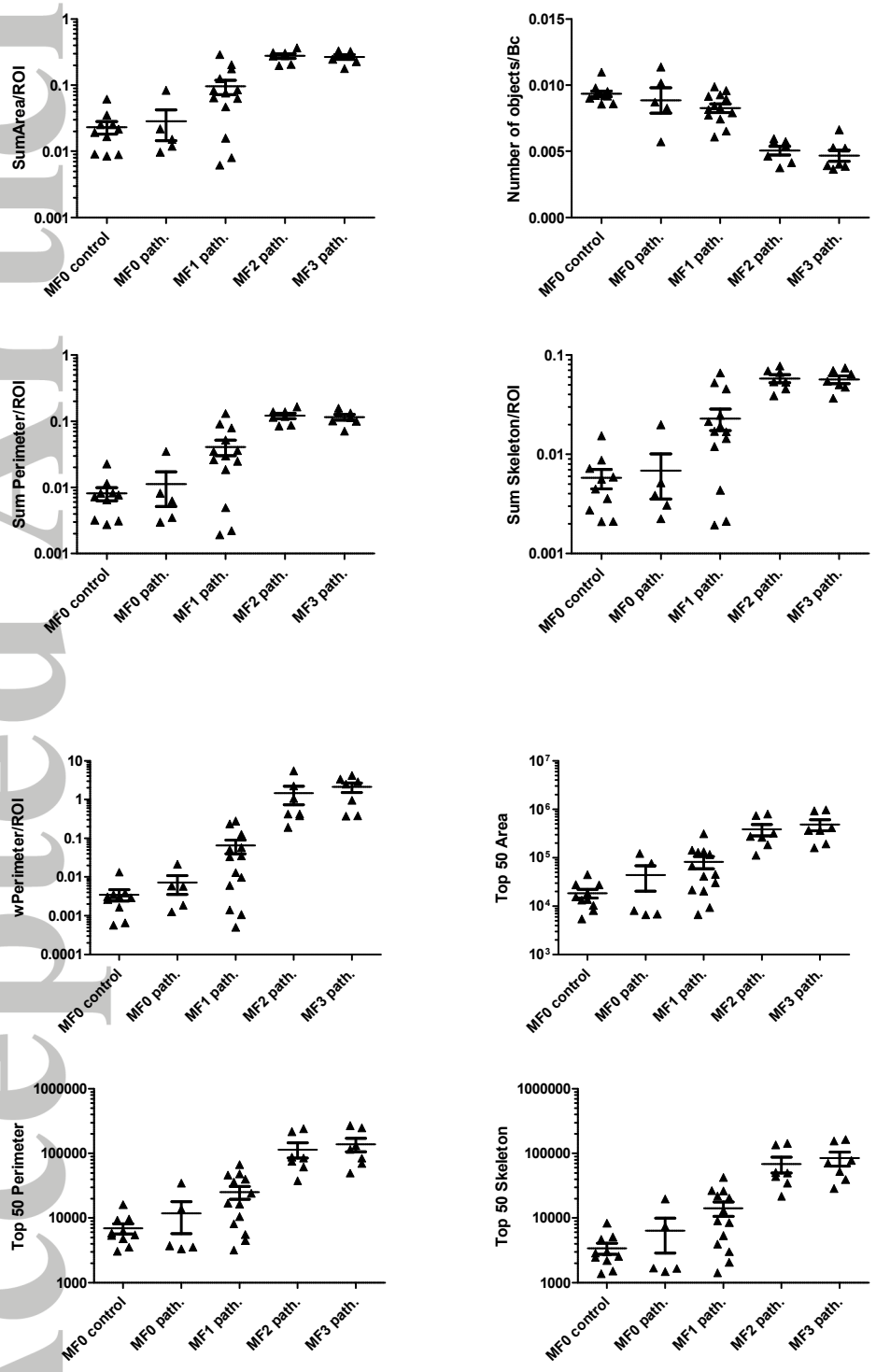

Figure 4.

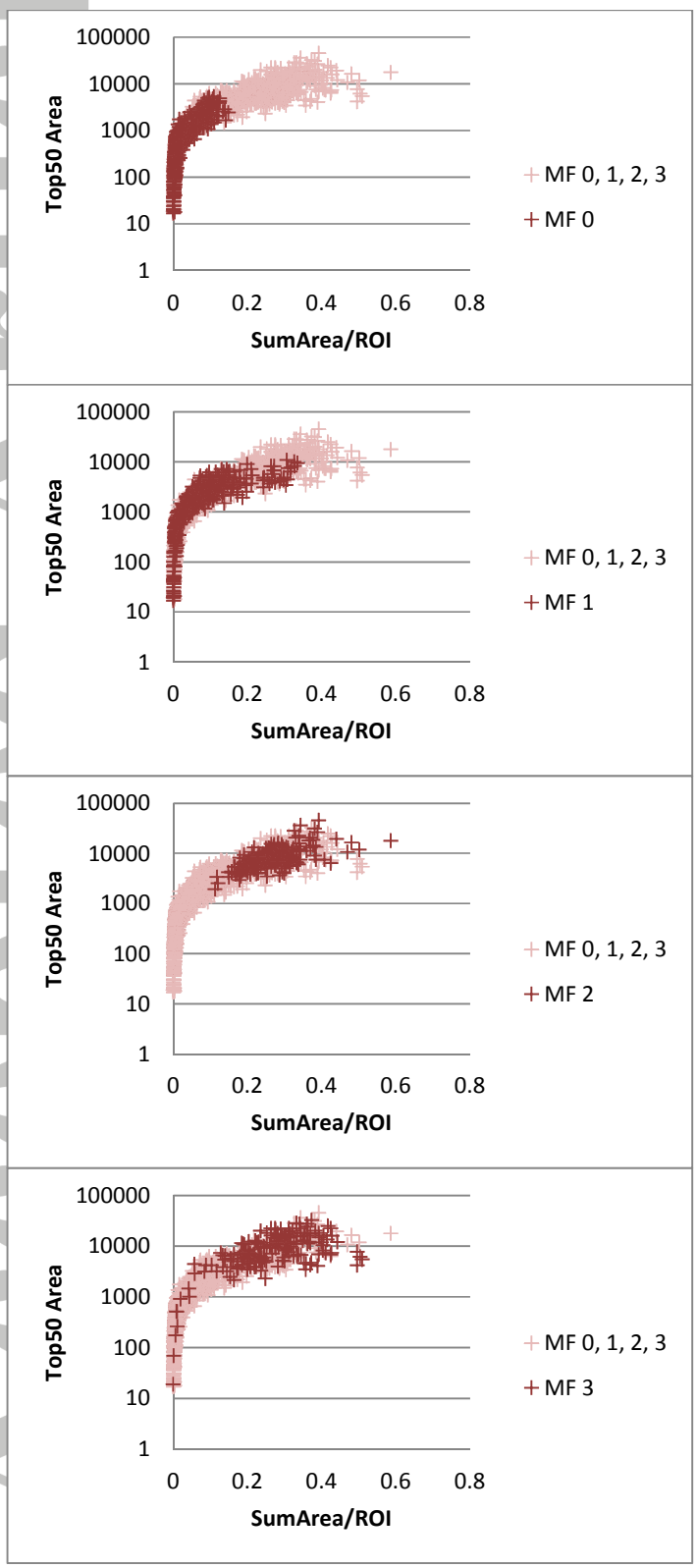

Figure 5.a case1

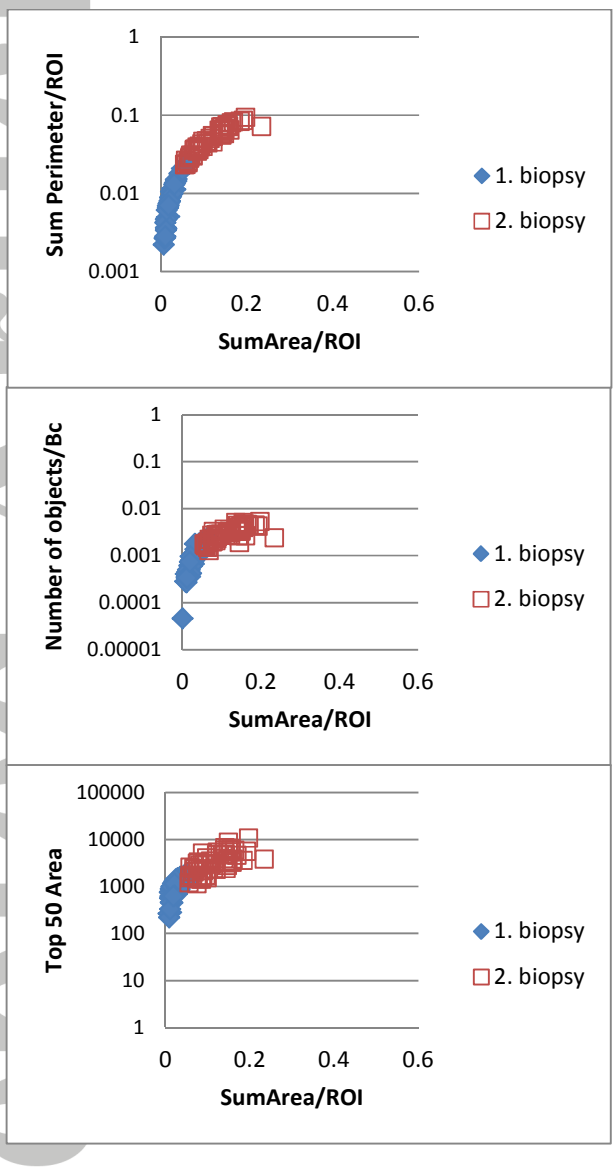

Figure 5.b case2